CrossMark
click for updates

# A high-throughput microfluidic single-cell screening platform capable of selective cell extraction†

Hyun Soo Kim,[a] Timothy P. Devarenne[b] and Arum Han*[ac]

Microfluidic devices and lab-on-a-chip technologies have been extensively used in high-throughput single-cell analysis applications using their capability to precisely manipulate cells as well as their microenvironment. Although significant technological advances have been made in single-cell capture, culture, and analysis techniques, most microfluidic systems cannot selectively retrieve samples off-chip for additional examinations. Being able to retrieve target cells of interest from large arrays of single-cell culture compartments is especially critical in achieving high-throughput single-cell screening applications, such as a mutant library screening. We present a high-throughput microfluidic single-cell screening platform capable of investigating cell properties, such as growth and biomolecule production, followed by selective extraction of particular cells showing desired traits to off-chip reservoirs for sampling or further analysis. The developed platform consists of 1024 single-cell trapping/culturing sites, where opening and closing of each trap can be individually controlled with a microfluidic OR logic gate. By opening only a specific site out of the 1024 trapping sites and applying backflow, particular cells of interest could be selectively released and collected off-chip. Using a unicellular microalga *Chlamydomonas reinhardtii*, single-cell capture and selective cell extraction capabilities of the developed platform were successfully demonstrated. The growth profile and intracellular lipid accumulation of the cells were also analyzed inside the platform, where 6–8 hours of doubling time and on-chip stained lipid bodies were successfully identified, demonstrating the compatibility of the system for cell culture and fluorescent tagging assays.

## Introduction

Single-cell assays are of great interest in many life science applications. Compared to conventional biological assays that measure the average response from a population of cells, single-cell analysis can provide information related to differences between individual cells, which allows for a more precise understanding of single-cell behavior as well as cell-to-cell differences. Single-cell resolution analysis is also important in the area of genetic/metabolic engineering or strain development in biotechnology applications where characteristics of each engineered/mutagenized cell have to be measured to find the desired cell traits of interest. Microfluidic devices and lab-on-a-chip technologies with their capability of precise

spatial and temporal control over samples or reagents at the single-cell level and their microenvironment, real-time monitoring and analysis, and high-throughput screening are ideal as high-throughput single-cell assay platforms.[1–3] Numerous microfluidic-based single-cell analysis techniques, including microwell arrays, dielectrophoresis, acoustophoresis, microscale physical trap arrays, hydrodynamic methods, and microdroplets have been developed and successfully utilized in a variety of applications, such as drug discovery, diagnostics, cancer research, systems and synthetic biology, bioenergy, and many other fields.[4–10]

In many single-cell assays, retrieving specific cells of interest among cell populations after analysis is necessary for target sample collection or further off-chip analysis. Drug screening is one good example; cells showing a certain trait (*e.g.*, drug resistance) can be extracted and analyzed further off-chip, which can improve the drug development processes.[11] Such targeted cell extraction is also essential when screening large engineered or mutagenized cell libraries in which mutants showing desired properties needs to be isolated, selectively collected off-chip, and re-grown.[12] We are particularly interested in applying microfluidic single-cell analysis platforms toward high-throughput screening of

[a] *Department of Electrical and Computer Engineering, Texas A&M University, College Station, Texas 77843, USA. E-mail: arum.han@ece.tamu.edu*
[b] *Department of Biochemistry and Biophysics, Texas A&M University, College Station, Texas 77843, USA*
[c] *Department of Biomedical Engineering, Texas A&M University, College Station, Texas 77843, USA*
† Electronic supplementary information (ESI) available: See DOI: 10.1039/c4lc01316f

engineered cell libraries, specifically mutagenized microalgal libraries in order to obtain the traits of improved productivity.[13–15]

Various microfluidic single-cell analysis platforms integrated with sorting capabilities have been developed.[16] Microfluidic flow cytometers and microdroplet-based microsystems are good examples, where large numbers of single cells or droplets containing a single cell can be analyzed and sorted.[5,8,16–19] Although these platforms have been successfully utilized in detecting and selectively sorting single cells at high-throughput, these are end-point measurements and thus cannot be used to track the exact same single cells over time (*i.e.*, lack of time-course analysis capabilities). Many of the platforms are also limited in single-cell culture capabilities and thus lack the capability to measure certain characteristics such as cell growth rate. Droplet microfluidic systems do have single-cell culture capabilities, but either do not allow long-term culture or require complicated droplet manipulation or processing to enable long-term culture.

Only a few microfluidic single-cell analysis platforms have been developed so far that allow both single-cell time-course analysis and selective cell retrieval capabilities. An optofluidic microsystem has been reported where single cells could be immobilized in a microwell array *via* sedimentation, and then selectively released using an infrared laser.[20] Hydrodynamic trapping schemes based on the principle of fluidic resistance have also been developed, where polymer beads or cell-encapsulating alginate beads captured at trapping sites could be selectively retrieved through an air bubble generated *via* laser heating.[21,22] However, both methods require expensive laser equipment as well as accurate alignment of the laser to each of the trapping sites. Negative dielectrophoresis (nDEP) combined with cell trapping *via* microdam structures or mild negative pressure in an array format has also been proposed.[23,24] However, this approach has low throughput, and would require complex on-chip interconnections and off-chip support circuitry, which would be unsuitable for large arrays of trapping sites. Most importantly, all of these cell trap designs are open-trap structures that do not have enough space for cell growth and division. As soon as cells divide and double, they will escape from the trapping sites, making it impossible to measure growth rates of individual cells.

In this study, we present a high-throughput microfluidic single-cell screening platform, which provides the capabilities of single-cell trapping in an array format ($32 \times 32 = 1024$ trapping sites), long-term culture and analysis of the cell's growth rates, on-chip fluorescent tagging, followed by selective retrieval of target cells showing traits of interest. The individual control of each trapping site using a microfluidic OR logic gate enabled selectively extracting only the cells of interest to off-chip reservoirs for further analysis or selection. The capabilities of the developed single-cell extraction platform were tested using a unicellular green microalga *Chlamydomonas reinhardtii*, a model microalga widely used for genetic and mutagenic engineering.

# Materials and methods

## Design and operating principle of the individually addressable single-cell trap

A platform that can screen through large libraries of cells such as genetically engineered or mutagenized cells requires the capability to capture and isolate single cells, culture the isolated single cells for some period of time while monitoring the cellular properties of interest, and to be able to selectively extract the cells of interest for collection or further analysis, all at high throughput. The microfluidic single-cell screening platform is composed of three poly(dimethylsiloxane) (PDMS) layers; a top microfluidic control layer, a middle microfluidic control layer, and a bottom microfluidic cell culture/analysis layer (Fig. 1A, ESI,† and Video S1). The bottom microfluidic cell culture/analysis layer (height: 16 μm) has an array of 1024 single-cell trapping sites ($32 \times 32$) where a single cell can be captured, cultured, and analyzed in each of the trapping sites with a continuous perfusion of culture media. After analysis, cells of interest residing in a particular trapping site can be selectively collected to an off-chip reservoir by opening only the particular trapping site while all other trapping sites remain closed, followed by applying backflow to release the cells from the selected trapping site (Fig. 1B–C). Each trapping site consists of a U-shaped microstructure (height: 16 μm, width: 15 μm) with a narrow opening (3 μm) in the center that functions as a single-cell trap and a top-hanging bar-shaped structure (height: 7 μm) that functions as a gate in front of the U-shaped cell trap (Fig. 2A). These gate structures at each trapping site can be individually controlled by utilizing the top and the middle control layers.

The top and the middle control layers have 32 columns and rows of control microchannels, respectively. When these two layers are combined together, 1024 junctions are generated in which each junction area matches with the gate structure of each trapping site in the underlying cell culture/analysis layer (Fig. 1A and 2A). Since a thin PDMS membrane (thickness: 20–25 μm) is formed between each layer, when hydraulic pressure is applied to the middle control microchannels, the thin membrane between the middle control layer and the underlying cell culture/analysis layer is pushed downward, which pushes down the gate structure (positioned 9 μm above from the bottom surface), closing the trapping site (Fig. 2E). On the other hand, if the hydraulic pressure is released from the middle control channels, the deformed membrane restores to its original position, lifting up the gate structure to open the trapping site (Fig. 2C). When the top control microchannels are actuated with hydraulic pressure, the thin PDMS membrane between the top and the middle control layer is pushed down, and consequently the ridge structures hanging upside down from the membrane pushes down the underlying PDMS membrane between the middle control layer and the cell culture/analysis layer together with the gate structure, closing the trapping site (Fig. 2D). To facilitate the closing of the gate structure when the top control layer is pressurized, a top-hanging ridge structure (3 μm
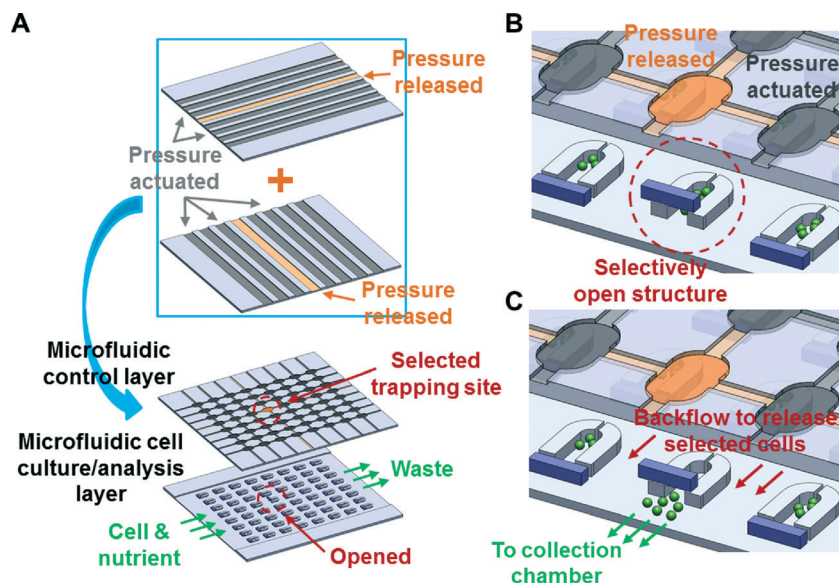
**Fig. 1** Illustration of the high-throughput microfluidic single-cell screening platform. (A) Two functional layers – a microfluidic control layer and a microfluidic cell culture/analysis layer. (B–C) Enlarged view of three U-shaped cell-trapping sites, each showing multiple cells grown from an initial single cell inside the traps. Bar-shaped gate structures in front of each U-shaped trap function as gates to control the opening and closing of each trapping site. The front gate is only open when pressure in both the row and column control microchannels in the control layer is released simultaneously. Trapped cells from only the cell trapping site with an open gate structure can be extracted when applying backflow.

above from the bottom) is employed in the middle control layer, which allows the closing of the trapping sites using lower hydraulic pressure.

Thus, the gate structure controlled by the two perpendicular control microchannels stacked on top of each other is designed to close the trap when either one of the top or the middle control microhannels are actuated with hydraulic pressure or when both microchannels are actuated with hydraulic pressure, but to remain open when neither microchannels are pressurized (Fig. 2C–F). The opening and closing principle of the cell trapping site is similar to a microfluidic OR logic gate (Fig. 2B). Here the output of the microfluidic OR logic gate becomes '0' (trapping site: open) only when both inputs to the gate are '0' (both control microchannels are "open", meaning no pressure applied). However, the output of the gate becomes '1' (trapping site: closed) if either one of the inputs or both are '1' (at least one of the two control microchannels are "closed", meaning pressurized). This microfluidic OR logic gate implemented here allows independently controlling a large array of trapping sites with minimum number of control lines.

### Independently accessing a large array of single-cell traps

To extract cells of particular interest, first, hydraulic pressure is applied to both the column-direction control microchannels in the middle control layer and the row-direction control microchannels in the top control layer, closing all trapping sites (Fig. 2D). Next, only the row (in the top control layer) and the column microchannels (in the middle control layer) covering the particular trapping site of interest are selected and then the hydraulic pressure is released, which

results in that particular trapping site to be opened while other trapping sites where either the row- or column-direction control microchannels are depressurized remain closed (Fig. 2E–F). Finally, by applying backflow from the outlet, cells from only this particular trapping site can be released and flow into an on-chip or off-chip reservoir for collection and further analysis (Fig. 1C and 2F).

To regulate each of the 32 control microchannels with reduced number of inputs, a microfluidic binary demulitplexer scheme was utilized in both the top and the middle control layers.[10,25] This allowed a total of 64 control microchannels to be regulated with only 22 inputs (10 for the binary demultiplexer control lines + 1 for input source = 11 inputs required for each of the top and the middle control layers). Thus, all of the 1024 trapping sites can be independently controlled and target cells of interest in any of the 1024 trapping sites can be selectively extracted using only 22 tubing connections. All control microchannels in both control layers were regulated by arrays of solenoid valves (SMC, Noblesville, IN) controlled by a custom LabView™ program (National Instruments, TX). All control microchannels were filled with DI water (hydraulic pressure) instead of air in order to prevent bubble formation in the cell culture/analysis layer during the operation.

### Microfabrication

The microfluidic platform was fabricated in PDMS (10:1 mixture, Sylgard® 184, Dow Corning, Inc., MI) using the soft-lithography technique.[26] The master molds for the top control layer, the middle control layer, and the bottom cell culture/analysis layer were fabricated by SU-8™ photoresist
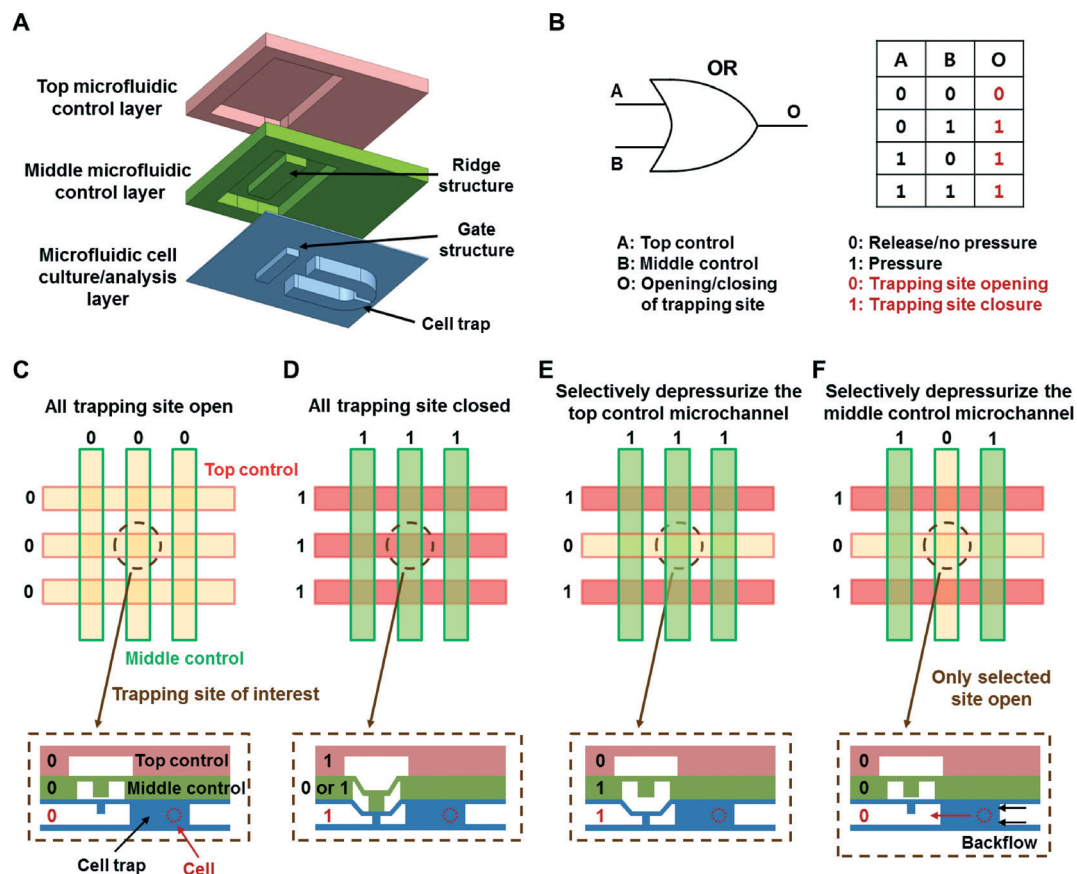
Fig. 2 Operation principle of a single trapping site and selective cell extraction process. (A) A schematic view of a U-shaped cell trap and a gate structure that can be selectively opened or closed using the two microfluidic control microchannels. (B) Actuation principle to close a single trapping site, which effectively becomes a microfluidic OR logic gate. (C) Selective cell extraction process from a particular trapping site. During cell loading, culturing, and analysis periods, all control microchannels in both control layers are not pressurized, and thus all trapping sites stay open. (D) To extract cells from a particular trapping site (highlighted with a dashed circle), first all trapping sites are closed by pressurizing all control microchannels. (E–F) By releasing the pressure from the second column-control microchannel in the top control layer (red) and the second row-control microchannel in the middle control layer (green), only the gate of the underlying trapping layer at the (2,2) position opens while all other traps remain closed. This allows selective release and collection of cells from the trap position (2,2) with backflow.

(Microchem, Inc., MA) using a conventional photolithography process. The top control microchannels and the binary demultiplexer for both control layers were 50 μm deep, obtained by spin-coating SU-8™ 2050 at 3500 rpm. The middle control microchannels with ridge structures were made of two SU-8™ layers by spin-coating them at 1000 and 3000 rpm, respectively (SU-8™ 2002: 3 μm, SU-8™ 2025: 30 μm). In the cell culture/analysis layer, the gate structures (thickness: 7 μm) were first patterned by spin-coating SU-8™ 2007 at 3500 rpm, followed by the fabrication of the U-shaped single-cell traps (thickness: 16 μm, SU-8™ 2015 at 3000 rpm). PDMS layers forming the top control microchannels (thickness: 70 μm, 1300 rpm), the middle control microchannels (thickness: 50 μm, 2000 rpm), and the cell culture/analysis layer (thickness: 40 μm, 2500 rpm) were replicated from the SU-8™ masters by spin-coating PDMS pre-polymer for 40 seconds. The thickness of the SU-8™ masters as well as the replicated PDMS devices was measured using an optical surface profilometer (Veeco NT9100, Veeco, NY) before assembly. All PDMS layers were aligned and assembled under a microscope

upon 90 seconds of exposure to oxygen plasma (Plasma cleaner, Harrick Plasma, NY). For sterilization, the assembled platform was treated with ultra-violet (UV) light for at least one hour. Prior to cell loading, this cell culture/analysis layer was also coated with bovine serum albumin (BSA) (VWR International, PA) for 3–5 hours by filling the microchannels with 3% (w/w) BSA solution to prevent cell adsorption as well as to minimize the background noise during Nile red staining.[10]

### Simulation of various single-cell trap designs

The cell trap for engineered or mutagenized cell library screening has two requirements. First it should have the capability to trap only a single cell with high efficiency, as each of the cells in the library are potentially different and should be tested for the trait of interest. Second, since the trait of interest can typically be only identified after some duration of culture (e.g., cell growth rate), meaning that multiple cells will be produced from a trapped single cell, it is

necessary to have a large-enough cell trap to allow room for cell growth and doubling. Three different trap designs have been proposed and tested (ESI†). All trapping sites consist of a U-shaped trapping structure of which the opening width, length, and overall height are 15, 62.5, and 16 μm, respectively. The first design has a 3 μm high supporting structure underneath the 13 μm high U-shaped cell trap. This supporting structure is employed to prevent the collapse of the cell trap as well as to maintain a small opening (width: 10 μm and height: 3 μm) at the center through which culture media or reagents can flow through (ESI).† The second design has the same schematic as the first design except for the width of the bottom supporting structure. Here the width of the supporting structure (12 μm) is narrower than that of the U-shaped cell trap (20 μm), resulting in more culture media flow through the cell trap, which would increase the possibility of cell capture (ESI†). The third design has a narrow opening (width: 3 μm, height: 16 μm) at the center of the U-shaped cell trap (height: 16 μm), as described in the previous section (ESI,† see 'Design and operating principle of the individually addressable single-cell trap').

Numerical simulations of fluidic flow through the three different trapping structures were conducted using a commercial finite element method (FEM) software (COMSOL Multiphysics®, COMSOL Inc., Los Angeles, CA, USA). To optimize the single-cell capturing efficiencies as well as backflow required for cell release, flow profiles inside each trap design for three situations – before cell capture, after cell capture, and during cell extraction, were simulated and compared. Next, the amount of fluid flowing through the gap (flow rate) in each trap design were characterized by calculating the average flow speeds as well as the cross-section of the gap in each design (flow rate = average flow speed passing through the cross section of the gap × cross sectional area of the gap).

### Cell preparation

The green unicellular microalga *Chlamydomonas reinhardtii* CC-125 strain was used as a model microorganism to demonstrate the functionality of the developed microfluidic platform. This strain was cultured in Tris-acetate-phosphate (TAP) media[27,28] at 23 °C under a light intensity of 100 μmol photons m$^{-2}$ s$^{-1}$ with a 12 hour light–dark cycle. *C. reinhardtii* was collected from an exponentially growing liquid TAP culture. To induce oil accumulation,[27,29] *C. reinhardtii* was grown in TAP media lacking NH$_4$Cl or any other N source (TAP-N) for 3–4 days before use.

### Functionality test of the developed microfluidic platform

*C. reinhardtii* cells were loaded into the cell culture/analysis layer with a syringe pump (Fusion 200, Chemyx Inc., Stafford, TX, 3–5 μl min$^{-1}$) to characterize the single-cell trapping efficiencies. Once all of the trapping sites were occupied with *C. reinhardtii* cells, any excessive microalgae were flushed out with fresh culture media (5–10 μl min$^{-1}$ for 10 minutes). Eight platforms were utilized to analyze the cell trapping

efficiencies by measuring the number of trapping sites with no cell, one cell, and more than two cells ($n = 8$). For validating the culture capability of the platform, *C. reinhardtii* cells inside the trapping sites were cultured under a light intensity of 100 μmol photons m$^{-2}$ s$^{-1}$ with a 12 hour light–dark cycle. Fresh TAP media was continuously perfused with a syringe pump at a flow rate of 1 μl min$^{-1}$. Fifty *C. reinhardtii* cells from 5 platforms were tested to analyze their cell doubling time by tracking the number of cells under a microscope ($n = 50$). For on-chip staining of lipid bodies within the *C. reinhardtii* cells, Nile red, a lipid-soluble fluorescent dye that binds to neutral lipids,[10,30,31] dissolved in dimethyl sulfoxide (DMSO) was diluted in TAP media to a concentration of 0.75 μg ml$^{-1}$ Nile red and 0.5% DMSO. This diluted solution was provided through the cell culture/analysis layer for 10 minutes at a flow rate of 1–10 μl min$^{-1}$, followed by rinsing with fresh media for 5 minutes. Microscopy for Nile red fluorescence (excitation: 460–500 nm, emission: 560–600 nm) as well as chlorophyll autofluorescence (excitation: 460–500 nm, emission > 610 nm) were conducted using a Zeiss Axio Observer Z1 microscope (Carl Zeiss Micro Imaging, LLC) equipped with a digital camera (Orca Flash2.8 CMOS Camera). A motorized stage as well as autofocusing and time-lapse imaging modules integrated in the microscope enabled tracking each of the 1024 trapping sites repeatedly. Automatic imaging of the whole platform could be achieved within 4 minutes. While testing the selective cell extraction process, the flow rate of the culture media was maintained at 1 μl min$^{-1}$ and 155 kPa of hydraulic pressure was applied to actuate the control microchannels in both the top and middle control layers. When extracting cells from a particular trapping site, a backflow was provided from the outlet at a flow rate of 3–5 μl min$^{-1}$. To characterize the success rate of the selective cell extraction, targeted cells from 35 different trapping sites in the platform were retrieved sequentially and its successful operation was evaluated (4 different platforms were tested, $n = 4$). Also, the viability of *C. reinhardtii* cells selectively retrieved from off-chip reservoirs of the platform after 24 hours of culture inside were verified by placing the extracted single cells into each well of a 96-well culture plate and monitoring their growth for 4 days under the same light condition described above (4 independent experiments were conducted, $n = 4$).

## Results and discussions

### Independent closing and opening of the single-cell trapping sites

Each of the 1024 trapping sites is open only when both control microchannels are not actuated with hydraulic pressure, but are otherwise closed if at least one of the control microchannels is pressurized. This working principle was tested and characterized by observing the lowering of the gate structure in each trapping site with incremental actuation pressure. First, when only the middle control microchannel was pressurized under a pressure of less than 90 kPa, the gate

structure was pushed down, but did not touch the bottom surface, thus the trap remained open (Fig. 3A). However, the trapping site was completely closed at a pressure of 90 kPa or higher, in which the overall gate structure tightly contacted the bottom surface (Fig. 3B, ESI† Fig. S1A, and ESI† Video S2, total deformation length required to fully close the trapping site: 9 μm).

When only the top control microchannel was actuated, a fairly high pressure of more than 360 kPa was required to fully close the trapping site. This is because the PDMS membrane between the top and the middle control layers had to be sufficiently pushed down to subsequently deform the underlying membrane between the middle control layer and the cell culture/analysis layer, which then lowered the blocking structure to close the cell trap (total deformation length required to fully close the trapping site: 30 (microchannel height in the middle control layer) + 9 = 39 μm). However, often this high pressure broke the bonding or damaged the PDMS membrane between the top and the middle control layers, making robust and repeated operation of the system a challenge. To reduce the required pressure (or the required deformation length) for the top control microchannel actuation, a 30 × 82 μm² ridge structure hanging upside down from the membrane and positioned 3 μm above the underlying membrane was utilized in the middle control microchannels (ESI† Fig. S1B). By employing this ridge structure, total Z-directional deformation length required was 12 μm (3 + 9 μm) and the trapping site could be completely closed with significantly lower actuation pressure of 155 kPa (Fig. 3B and ESI† Video S3). This significantly lower actuation pressure compared to the previous 360 kPa significantly increased the system stability by minimizing the membrane damage. Thus, successful closing and opening of the gate structure through actuating the top and the middle control microchannels enabled a microfluidic OR logic gate (ESI† S4–S5). Thus a pressure of 155 kPa was used in all subsequent experiments.

## Single-cell trapping efficiency

To estimate the trapping efficiency and backflow required to release cells, fluidic flow profiles (flow rate, defined as the amount of fluid passing through the gap cross-section per unit time (m³ s⁻¹)) inside the three different trapping sites were analyzed and compared through numerical simulation (ESI†). Based on flow rate changes before and after capturing cells, the first design would have the highest single-cell trapping efficiency as less amount of fluid will flow through this trap design once the trapping sites are occupied (60% flow reduction), compared to the other two designs (second − 14%, third − 40% flow reduction), resulting in the least probability in capturing more than two cells in a single trap. Fluid flow during the cell extraction process (i.e., when applying backflow to release cells) was also analyzed with a captured cell inside. The highest flow rate and the lowest flow rate were observed from the second and the first designs, respectively, meaning that more backpressure will be required for the first design to achieve the same degree of backflow compared to other two designs. For example, approximately 2.3 and 1.5-fold of backflow is required in the first design to obtain the same amount of fluid flow as the second and the third designs. Based on these simulation results, the first design will have the highest single-cell trapping efficiency, but will require more backflow during the cell extraction process. The second design will need the least backflow to release cells from the cell trap, but will have the lowest single-cell trapping efficiency. The third design will have a slightly lower trapping efficiency compared to the first design, but will require much less backflow to extract the cells for off-chip analysis. Considering these simulation results, the third trapping design was selected and utilized in the microfluidic single-cell screening platform (more details are described in ESI†).

Trapping efficiency of the selected trapping structure design (third design) was then evaluated experimentally by
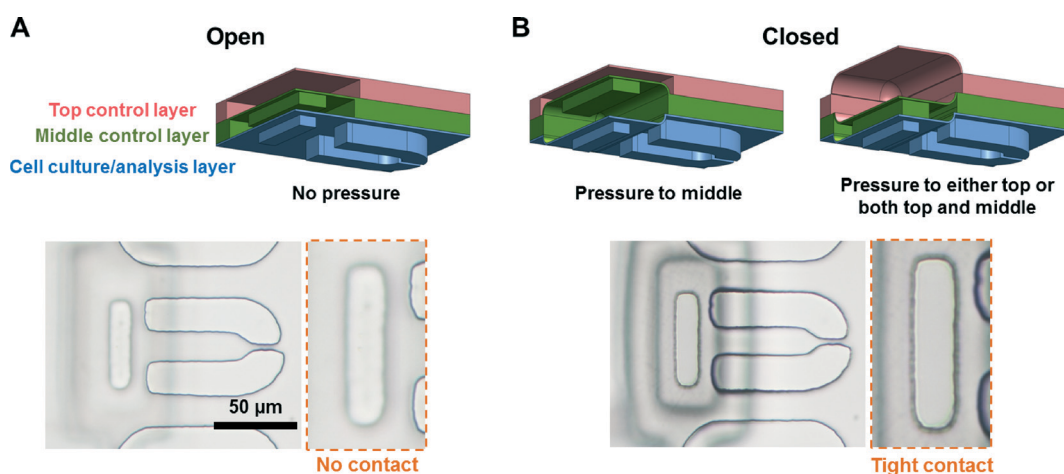


**Fig. 3** Microscopic images showing the opening and closing of the trapping site. (A) Trapping site remaining open, where the gate structure had no contact with the bottom surface of the cell culture/analysis layer. (B) Trapping site closed as the gate structure formed a tight contact with the bottom surface. Inset images (orange dashed line) show the enlarged view of the gate structure.

measuring the number of trapping sites having no cell, one cell, and more than two cells. The third trapping structure design had an overall cell trapping efficiency of 91.8 ± 2.9% (average ± standard deviation), where 7.7 ± 2.6% sites were empty, 8.7 ± 5.1% sites had more than two cells captured, and 83.2 ± 3.4% had only a single cell trapped (ESI† Fig. S2, $n = 8$).

## Capability of culturing and staining microalgae

The culture capability of the platform was tested by growing *C. reinhardtii* inside the platform. Fig. 4A shows single-cell level behavior of *C. reinhardtii*, such as cell size increase and cell division, after being captured in the cell trap. This micro-alga was observed to undergo 2–4 rounds of mitosis before daughter cells are divided and separated from a mother cell (ESI† Video S6).[27] The doubling time of *C. reinhardtii* inside the platform was determined to be 6–8 hours ($n = 50$), which was consistent with previous studies using conventional flask systems.[32] The on-chip fluorescence staining capability of the platform was also characterized. Fig. 4B shows microscopic images of oil bodies successfully stained with Nile red (yellow) and autofluorescence from chlorophyll (red, biomass indicator), demonstrating the on-chip analysis capability of the developed platform.

The capabilities of culturing and analyzing cells are essential requirements for the developed system to be used as a cell screening platform. Compared to conventional culture systems (lab-scale flasks), the developed single-cell screening platform has several advantages. In the microfluidic single-cell screening platform, the growth profile of *C. reinhardtii* can be obtained with single-cell resolution. In addition, identical light exposure conditions could be applied in the developed platform unlike the conventional culture systems that are hampered by light blocking problems caused by self-shading. Thus, information obtained through this platform is consistent and could be used in mechanistic studies that require accurate and consistent cellular microenvironment.

## Selective cell extraction

Fig. 5A shows successful release of a *C. reinhardtii* cell from a target trapping site with backflow. Selective cell extraction was demonstrated next. As shown in Fig. 5B–D, only a particular trapping site ($S_{3,2}$) was opened out of the 1024 sites by releasing pressure from the top control microchannel $T_2$ and the middle control microchannel $M_3$, which allowed only the *C. reinhardtii* cell inside this particular trapping site to be extracted to an off-chip reservoir without affecting cells captured in other trapping sites (Fig. 5D).

This process could be repeated to sequentially release cells from other trapping sites of interest. For example, all trapping sites were closed again when all microchannels in both
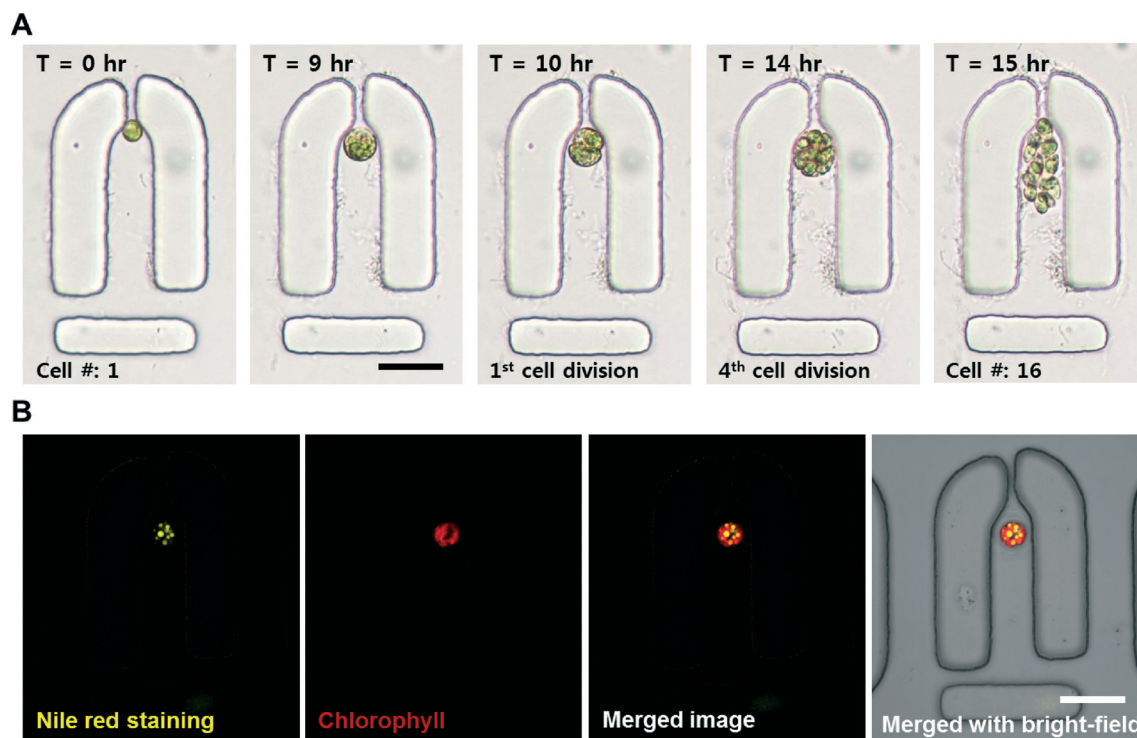


**Fig. 4** Microscopic images showing culture and on-chip staining capabilities of the platform. (A) Single-cell resolution growth profile of *C. reinhardtii* showing size increase, followed by cell division inside the cell trap over a 15 hour period. (B) Oil accumulation in *C. reinhardtii* grown under N-limited condition was analyzed inside the cell trap through Nile red fluorescenct dye staining. Chlorophyll autofluorescence (red) indicates biomass and Nile red staining (yellow) shows lipid content. Scale bar = 25 μm.
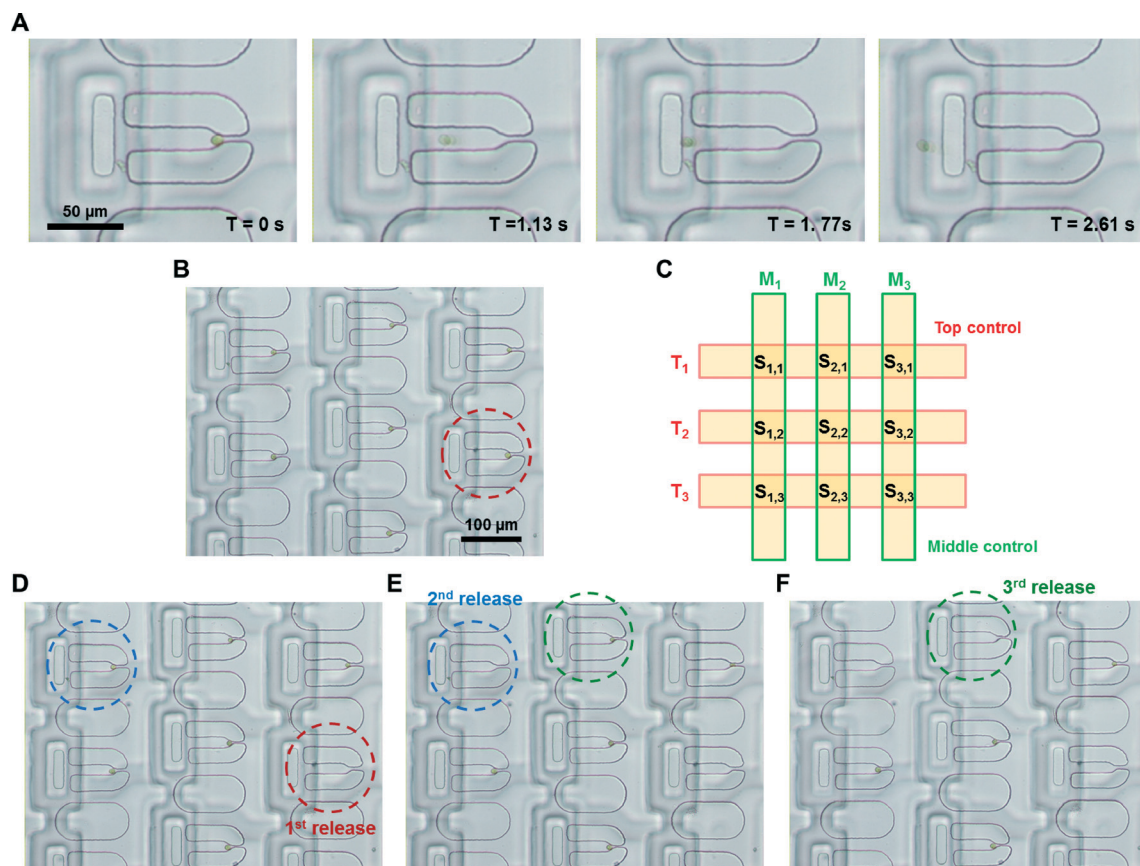
**Fig. 5** Microscopic images showing selective cell extraction from a particular trapping site of interest. (A) Time-lapse images showing a cell from site $S_{1,1}$ being released when backflow was applied. (B) Before extracting cells, all trapping sites were closed. (C) Illustration showing 3 top and 3 middle control microchannels on top of 9 single-cell trapping sites ($S_{1,1}$–$S_{3,3}$). (D) By selectively releasing pressure from the $M_3$ and $T_2$ control microchannels, a cell captured at trapping site $S_{3,2}$ was successfully released. (E–F) By releasing pressure only from the chosen top and middle control microchannels on top of the target trapping sites, cells inside the target site could be released without affecting other trapping sites.

control layers were pressurized after releasing the cell from position $S_{3,2}$ (Fig. 5D). Then, a second cell trapping site ($S_{1,1}$) was selectively opened by releasing pressure from the top and the middle control microchannels ($T_1$ and $M_1$) controlling this trapping site, and the *C. reinhardtii* cell could be successfully released once backflow was applied (Fig. 5E). This process was repeated for trapping site $S_{2,1}$ (Fig. 5F) by releasing pressure from the microchannel $T_1$ and $M_2$. The overall operation of the selective cell extraction is visualized in ESI† Video S7.

The success rate of the selective cell extraction process was evaluated by sequentially retrieving *C. reinhardtii* cells from 35 different trapping sites in the platform (ESI† Fig. S2). From 4 different platforms tested, 97.9 ± 2.7% success rate was obtained (ESI† Fig. S2G, $n = 4$). However, even in failure situations, these failed trapping sites always had cell debris or other material, resulting in the cell itself being stuck in the PDMS device, not from the operation of the platform (ESI† Fig. S2E–F). The viability of *C. reinhardtii* cells selectively retrieved from the platform was also characterized where 98.9 ± 0.9% of cells placed in a 96-well culture plate showed growth and the same doubling time (6–8 hours) observed in the microfluidic platform (ESI† Fig. S3, $n = 4$).

## Conclusion

We have developed a microfluidic high-throughput single-cell screening platform with the capability of capturing, culturing, and analyzing cells with single-cell resolution, followed by selectively extracting particular cells of interest off-chip for further study. Two microfluidic control layers regulated by a binary demultiplexer scheme and a microfluidic OR logic gate enabled independent control of the opening and closing of each of the 1024 trapping sites with much reduced complexity. By opening only a particular trapping site while others remained all closed, cells of interest could be successfully retrieved among cell populations in the platform by applying backflow. The growth profile of a captured single *C. reinhardtii* cell was monitored over time and its oil accumulation was also analyzed through on-chip Nile red fluorescent lipid staining. Finally, single *C. reinhardtii* cells from a particular trapping site were successfully isolated and extracted to an off-chip reservoir (98% of success rate) where 99% of retrieved cells showed viability. We expect that this system will serve as a powerful high-throughput single-cell screening and analysis tool in broad ranges of applications where screening through large libraries of genetic variants is needed.

# Acknowledgements

# References

1 G. M. Whitesides, *Lab Chip*, 2011, **11**, 191–193.

2 G. B. Salieb-Beugelaar, G. Simone, A. Arora, A. Philippi and A. Manz, *Anal. Chem.*, 2010, **82**, 4848–4864.

3 D. Mark, S. Haeberle, G. Roth, F. von Stetten and R. Zengerle, *Chem. Soc. Rev.*, 2010, **39**, 1153–1182.

4 H. Yin and D. Marshall, *Curr. Opin. Biotechnol.*, 2012, **23**, 110–119.

5 S. Lindstrom and H. Andersson-Svahn, *Lab Chip*, 2010, **10**, 3363–3372.

6 V. Lecault, A. K. White, A. Singhal and C. L. Hansen, *Curr. Opin. Chem. Biol.*, 2012, **16**, 381–390.

7 S. Y. Teh, R. Lin, L. H. Hung and A. P. Lee, *Lab Chip*, 2008, **8**, 198–220.

8 T. P. Lagus and J. F. Edd, *J. Phys. D: Appl. Phys.*, 2013, **46**, 114005.

9 A. Han, H. Hou, L. Li, H. S. Kim and P. de Figueiredo, *Trends Biotechnol.*, 2013, **31**, 225–232.

10 H. S. Kim, T. L. Weiss, H. R. Thapa, T. P. Devarenne and A. Han, *Lab Chip*, 2014, **14**, 1415–1425.

11 M. J. Marton, J. L. DeRisi, H. A. Bennett, V. R. Iyer, M. R. Meyer, C. J. Roberts, R. Stoughton, J. Burchard, D. Slade and H. Dai, *Nat. Med.*, 1998, **4**, 1293–1301.

12 M. H. Huesemann, T. S. Hausmann, R. Bartha, M. Aksoy, J. C. Weissman and J. R. Benemann, *Appl. Biochem. Biotechnol.*, 2009, **157**, 507–526.

13 S. A. Scott, M. P. Davey, J. S. Dennis, I. Horst, C. J. Howe, D. J. Lea-Smith and A. G. Smith, *Curr. Opin. Biotechnol.*, 2010, **21**, 277–286.

14 D. R. Georgianna and S. P. Mayfield, *Nature*, 2012, **488**, 329–335.

15 Y. Chisti, *J. Biotechnol.*, 2013, **167**, 201–214.

16 J. Autebert, B. Coudert, F. C. Bidard, J. Y. Pierga, S. Descroix, L. Malaquin and J. L. Viovy, *Methods*, 2012, **57**, 297–307.

17 D. Huh, W. Gu, Y. Kamotani, J. B. Grotberg and S. Takayama, *Physiol. Meas.*, 2005, **26**, R73–98.

18 T. Sun and H. Morgan, *Microfluid. Nanofluid.*, 2010, **8**, 423–443.

19 L. Mazutis, J. Gilbert, W. L. Ung, D. A. Weitz, A. D. Griffiths and J. A. Heyman, *Nat. Protoc.*, 2013, **8**, 870–891.

20 J. R. Kovac and J. Voldman, *Anal. Chem.*, 2007, **79**, 9321–9330.

21 W. H. Tan and S. Takeuchi, *Proc. Natl. Acad. Sci. U. S. A.*, 2007, **104**, 1146–1151.

22 W. H. Tan and S. Takeuchi, *Lab Chip*, 2008, **8**, 259–266.

23 B. M. Taff, S. P. Desai and J. Voldman, *Appl. Phys. Lett.*, 2009, **94**, 84102.

24 Z. Zhu, O. Frey, D. S. Ottoz, F. Rudolf and A. Hierlemann, *Lab Chip*, 2012, **12**, 906–915.

25 T. Thorsen, S. J. Maerkl and S. R. Quake, *Science*, 2002, **298**, 580–584.

26 Y. Xia and G. M. Whitesides, *Annu. Rev. Mater. Sci.*, 1998, **28**, 153–184.

27 E. H. Harris, D. B. Stern and G. Witman, *The chlamydomonas sourcebook*, Cambridge Univ Press, 2009, vol. 2.

28 D. S. Gorman and R. P. Levine, *Proceedings of the National Academy of Sciences*, 1965, **54**, 1665–1669.

29 E. R. Moellering and C. Benning, *Eukaryotic Cell*, 2010, **9**, 97–106.

30 D. Elsey, D. Jameson, B. Raleigh and M. J. Cooney, *J. Microbiol. Methods*, 2007, **68**, 639–642.

31 T. L. Weiss, H. J. Chun, S. Okada, S. Vitha, A. Holzenburg, J. Laane and T. P. Devarenne, *J. Biol. Chem.*, 2010, **285**, 32458–32466.

32 Y. Lee do and O. Fiehn, *Plant Methods*, 2008, **4**, 7.